TBK1 mutations cause amyotrophic lateral sclerosis and fronto-temporal dementia

Axel Freischmidt[1,*], Thomas Wieland[2,*], Benjamin Richter[3,*], Wolfgang Ruf[1,*], Veronique Schäffer[3,*], Kathrin Müller[1], Nicolai Marroquin[1,12], Frida Nordin[4], Annemarie Hübers[1], Patrick Weydt[1], Susana Pinto[5], Rayomond Press[6], Johannes Dorst[1], Elisabeth Graf[2], Thomas Meyer[7], Andrea S. Winkler[8], Juliane Winkelman[8], Mamede de Carvalho[9], Dietmar R. Thal[10], Markus Otto[1], Thomas Brännström[11], Alexander E. Volk[12,15], Pourya Sarvari[16], Didier Y.R. Stainier[16], Petri Kursula[13], Karin M. Danzer[1], Peter Lichtner[2], Ivan Dikic[3], Thomas Meitinger[2,14], Albert C. Ludolph[1], Tim M. Strom[2,14,*], Peter M. Andersen[1,4,*], Jochen H. Weishaupt[1*]

(1) Department of Neurology, Ulm University, Ulm, Germany,
(2) Institute of Human Genetics, Helmholtz Zentrum München, Neuherberg, Germany
(3) Institute of Biochemistry II, Goethe University Medical School, Frankfurt, Germany
(4) Department of Pharmacology and Clinical Neurosience, Umeå University, Umeå, Sweden
(5) Institute of Physiology and Institute of Molecular Medicine, University of Lisbon, Lisbon, Portugal
(6) Department of Neurology, Karolinska Hospital Huddinge, Stockholm, Sweden
(7) Charité University Hospital, Humboldt-University, Berlin, Germany
(8) Department of Neurology, Technical University of Munich, Munich, Germany
(9) Department of Neurosciences, Hospital de Santa Maria-CHLN, Lisbon, Portugal
(10) Institute of Pathology – Laboratory of Neuropathology, Ulm University, Ulm, Germany
(11) Department of Medical Biosciences, Umeå University, Umeå, Sweden
(12) Institute of Human Genetics, Ulm University, Ulm, Germany
(13) University of Oulu Biocenter, Faculty of Biochemistry and Molecular Medicine, Oulu, Finland
(14) Institute of Human Genetics, Technische Universität München, Munich, Germany
(15) Institute of Human Genetics, University Clinic Hamburg-Eppendorf, Hamburg, Germany
(16) Max Planck Institute for Heart and Lung Research, Dpt. III – Developmental Genetics, Bad Nauheim, Germany
(*) Shared authorships

Corresponding authors: Prof. Dr. Jochen H. Weishaupt
Ulm University
Department of Neurology
Albert-Einstein-Allee 11
89081 Ulm
Germany
Email: jochen.weishaupt@uni-ulm.de
Phone: +49 – (0)731 50063073

Prof. Dr. Peter M. Andersen
Department of Clinical Neuroscience
Umeå University
901 87 Umeå
Sweden
Email: peter.andersen@umu.se
Phone: + 46 90 785 23 72

Introductory paragraph

Amyotrophic lateral sclerosis (ALS) is a neurodegenerative disorder hallmarked by adult-onset loss of motor neurons and fatal paralysis[1]. Here, we show that mutations in the gene encoding TANK-binding kinase 1 (*TBK1*) cause ALS and fronto-temporal dementia (FTD). By exome sequencing of 202 familial ALS patients and 827 control individuals, we found an exome-wide significant enrichment of *TBK1* loss-of-function (LoF) mutations in the patient group. Another 4 LoF mutations were identified during a subsequent targeted screening of 1076 additional patients. *TBK1* mutations co-segregated with disease in five families with reduced penetrance. Genetic and biochemical data suggested a critical role for the C-terminal TBK1 coiled coil domain (CCD) that mediates binding to the TBK1 adaptor protein optineurin in neurodegeneration. A mild knock-down of *TBK1* expression in zebrafish caused shortening and abnormal branching of motor neurons *in vivo*. We conclude that haploinsufficiency of *TBK1* causes ALS and dementia/FTD.

Main text

Mutations in 29 genes have been linked to ALS pathogenesis[2,3] and are frequently also associated with fronto-temporal dementia (FTD). However, mutations in known ALS genes explain less than 1/3 of ALS cases [2,3].

To evaluate low-frequency variants in protein-coding genes DNA samples from 202 familial ALS (fALS) patients were selected for exome sequencing. They had been previously screened negative for *SOD1* and *C9orf72* mutations and came from families with two or more affected individuals per family from the Nordic countries, Germany and Portugal. Control exomes (n=827) from Germany were used to compare the variant burden. We used a gene-based test (CMC test,[4]) to analyze all missense variants at four MAF thresholds (MAF <= 5%, 1%, 0.1% and 0.05%). In addition, LoF variants defined as nonsense, canonical splice site (within two nucleotides of exon boundary), read-through and frameshift variants were investigated separately (MAF <= 5%). While analysis of missense variants revealed no prominent hits (**Supplementary Fig. 1**), the test for LoF variants revealed two outliers, *TBK1* and *IL1RL1*, with p-values of 4.048e-7 and 6.982e-9, respectively (**Supplementary Fig. 1**). *IL1RL1* proved to be a sequencing artifact in a low complexity region, leaving *TBK1* as the only candidate. LoF variants in *TBK1* were absent in controls, whereas ALS patients carried 7 different LoF mutations in 8 individuals (**Table 1, Table 2 and Supplementary Table 1**).

For further evaluation of *TBK1* variation, we screened in a second stage additional case and control groups using a targeted high resolution melting curve protocol including 50 fALS and 516 sporadic ALS (sALS) patients from Sweden, 510 German sALS cases as well as 650 Swedish control subjects. A splice site variant was detected in a Swedish fALS patient and another splice site variant was present in 3 sALS patients from Sweden and one control individual.

Clinically, patients carrying TBK1 LoF mutations had a median age of onset of 61 years, 45% showed cognitive impairment often progressing to fulminant FTD, and bulbar onset was observed in 36%. **Table 1** provides an overview of all identified *TBK1* variants. It includes TBK1 variants from additional 1,791 in-house exomes and 63,358 exomes of the ExAC public dataset [5](**Table 1 and Supplementary Table 1**). Accordingly, *TBK1* is highly conserved: it does only contain a single variant with a MAF larger than 1%. All other 171 non-synonymous variants had a MAF smaller than 0.1%. The presence of 8 LoF variants in the ExAC dataset was higher than expected when assuming a lifetime risk for ALS of approximately 1 in 450 according to normal population registries [6,7]. This is most likely explained by the fact that the ExAC dataset is not representative for the general population but contains disease-specific samples from various exome sequencing projects [5] including schizophrenia, which has been clinically linked to ALS [8].

Co-segregation with ALS or dementia was found in 5 families, confirming causative linkage of *TBK1* LoF mutations with ALS (**Fig. 1a–f**): TBK1 mutations co-segregated with disease between 2 cousins in

a Danish Family (**Fig. 1a**), two second degree relatives in a Swedish family (**Fig. 1b**), as well as between 4 first degree relatives in a German family (**Fig. 1c**). The identical splice site mutation (p.690-713del) was found in a Danish and a Swedish Family but not in over 70 000 controls (**Fig. 1e and f**). This prompted us to undertake genealogical investigations and indeed we could track both families to a common ancestor in Sweden 5 generations earlier (**Fig. 1e and f**).

Investigation of unaffected individuals provided evidence for reduced penetrance. In family 3 (**Fig. 1b**), the p.Ile450LysfsX14 mutation was observed in 3 unaffected individuals who survived the latest known onset of disease observed in this family by 11, 14 or 21 years. We also found *TBK1* LoF mutations in 3 patients who had no reported family history of ALS (**Table 2**). This is consistent with incomplete penetrance and the same pattern has also been found for other ALS mutations in the *SOD1, C9orf72, FUS, ANG, TDP43, OPTN and p62* genes [2].

In family 5 (**Fig. 1c**) a maternally transmitted TBK1(p.Tyr185X) nonsense mutation was observed together with a paternal FUS(p.R524G) missense mutation. The *TBK1* mutation was associated with dementia in the index patient's mother and the *FUS* mutation with ALS in her father (**Fig. 1c**). The relative contribution of each variant, both co-segregating with disease in the following generation, cannot be determined at this point. However, this observation supports the notion of an oligogenic basis of ALS which has previously been reported for other ALS mutations [9].

Taken together, the highly significant increase in LoF mutational burden in ALS together with co-segregation with disease demonstrates causality of the identified TBK1 LoF mutations. Consequently, we investigated selected mutations *in vitro* and *in vivo* in order to clarify the pathogenic mechanisms. Most LoF mutations seemed to result in haploinsufficiency. In a patient–derived immortalized lymphoblast cell line the splice site mutation c.358+2T>C (p.Thr77TrpfsX3) resulted in a low expression of an aberrant splice product the mRNA level, most likely as a consequence of nonsense-mediated RNA decay, without compensatory upregulation of the wild-type allele at the mRNA or protein level (**Supplementary Fig. 2**). The same mutation expressed in neuronal H4 cells did not result in subcellular re-distribution or aggregation of TBK1 (**Supplementary Fig. 3**). Faint immunohistochemical staining intensities of the truncating LoF mutants were in agreement with the low expression levels observed by Western blotting (**Fig. 2a and f**).

To determine if a subset of the identified missense variants also resulted in a loss-of-function, we investigated their kinase activity and ability to bind to substrate and adaptor proteins. Several rare missense variants identified in our screens were predicted to impair TBK1 function based on the analysis of the TBK1 crystal structure (**Supplementary Fig. 4** and [10]). p.M559 is predicted to be buried in a hydrophobic pocket of the scaffold/dimerization domain (amino acids 408–654) and its substitution by an arginine to result in a disturbed protein structure (**Supplementary Fig. 4** and [10]). p.M559R indeed resulted in a complete loss of optineurin (**Fig. 2a-c**) and interleukin-related factor 3

(IRF3) binding (**Fig. 2e**), a loss of TBK1 kinase activity (**Fig. 2d and f**), and loss of IRF3 activation (**Figure 2f and g**). p.M559R is thus likely to result in loss-of-function while the causal relevance of the other rare missense variants (**Fig. 2**) with the exception of p.E696K (see below) cannot be adequately judged at this point. A mild knock-down of the *TBK1* zebrafish orthologue resulted in shortening and abnormal branching of motor neuron axons, further supporting a *TBK1* LoF mechanism *in vivo* (**Fig. 3**). Taken together, our data indicate that most pathogenic variants identified represent null mutations, and dosage reduction from 2 copies to a single *TBK1* copy is sufficient to cause ALS or FTD**.**

In contrast to the 6 different truncating mutations found in ALS cases (**Table 2**), the c.2138+2T>C splice site mutation co-segregating in the extended Danish/Swedish pedigree over 9 generations (**Fig. 1e**) is predicted to result in exon skipping and in-frame deletion of 24 amino acids in the C-terminal coiled-coil domain (CCD) of TBK1 (p.690-713del). This domain was shown to mediate the binding to various adaptor proteins relevant for TBK1 activation [11]. A point mutation in the same CDD (p.E696K) was associated with a similar clinical phenotype of progressive bulbar palsy and a disease duration of less than 2 years in two different families, supporting causality for this point mutation. Haplotype analysis was compatible with a common founder in both families (**Supplementary Fig. 5**). Therefore, the absence or mutation of the C-terminal adaptor-binding CCD of TBK1 seems to be sufficient to induce neurodegeneration. Staining of the brain of patient III/3 (**Fig. 1e**) with the p.690-713del mutation revealed Type B TDP-43 positive perinuclear inclusion in neurons in lamina III of the temporal lobe and p62 positive perinuclear inclusions in lamina III in the right para-hippocampal gyrus (**Supplementary Fig. 6**).

Both p.690-713del and p.E696K abolished binding to the prototypic TBK1 adaptor protein optineurin (**Fig. 2a-c**). However, binding to (**Fig. 2e**) and activation (**Figure 2f and g**) of IRF3 was unaffected upon overexpressin. IRF3 is a TBK1 substrate that binds to the more upstream ubiquitin-like domain (ULD) of TBK1 [12]. The p.E696K mutation we have identified in ALS patients has been employed before as an (at that time) “artificial” mutation to dissect the structure/binding properties of the TBK1 C-terminal CCD [11]. In contrast to the observed loss of optineurin binding (**Fig. 2a-c**), normal binding of TBK1(p.E696K) to other TBK1 adaptor proteins such as TANK, Sintbad and NAP1 was observed [11]. These findings point to the relevance of the disruption of the CCD for disease causation and suggest that loss of TBK1/optineurin interaction is associated with the development of neurodegeneration.

In summary, we demonstrate that *TBK1* haploinsufficiency causes ALS and fronto-temporal dementia. As the frequency of *TBK1* LoF mutations was 4% in our exome-sequenced cohort of 202 genetically unexplained fALS index patients, *TBK1* mutations may be one of the more common genetic causes of ALS among Caucasians. Moreover, our genetic and functional data point to a critical role of the C-terminal TBK1 adaptor-binding domain and its interaction with optineurin as a cause of

neurodegeneration. Earlier studies reported mutations in optineurin [13] and p62/SQSTM1 [14], which are both autophagy regulating adaptor proteins and substrates of TBK1 [15,16], as possible causes of ALS. The present results link three ALS-FTD associated genes to a common pathway.

Table 1. TBK1 variants with the respective allele frequencies.

	Variants	Cases (exomes)	Cases (HRMC[a])	Controls (HRMC[a])	Controls (in-house exomes)	Controls (ExAC)
n	189	202	1076	650	2,663	63,358
LoF	13	8 (2.0%)	4 (0.2%)	1 (0.1%)	0	8 (0.0%)
Inframe indel	4	0	2 (0.1%)	0	0	48 (0.0%)
missense MAF<=5% and >1%	1	11 (2.7%)	70 (3.3 %)	34 (2.6 %)	105 (2.0%)	1,653 (1.3%)
missense MAF<=1% and >0.1%	0	0	0	0	0	0
missense MAF<=0.1%	171	4 (1.0%)	13 (0.6%)	4 (0.3%)	28 (0.5%)	781 (0.6%)

[a]High resolution melting curve analysis.

Table 2. List of all loss-of-function mutations and rare missense variants (MAF < 0.0001) detected in ALS patients.

Type of variant	**Variant**	**Predicted consequence at protein level**	**Index patient (if respective pedigrees is displayed in Fig. 1)**	**Family**	**fALS/ sALS**	**Country**	**Detection method: exome sequencing or HRMCA**
Loss-of-function mutations	958_958delA	p.Thr320GlnfsX39	-	family 1	fALS	Sweden	ES
	c.1343_1346delAATT	p.Ile450LysfsX14	III/1 (Fig. 1a)	family 2	fALS	Denmark	ES
	c.1343_1346delAATT	p.Ile450LysfsX14	III/2 (Fig. 1b)	family 3	fALS	Sweden	ES
	c.1434_1435delTG	p.Val479GlufsX3	-	family 4	fALS	Sweden	ES
	c.555T>A	p.Tyr185X	III/5 (Fig. 1c)	family 5	fALS	Germany	ES
	c.358+2T>C	p.Thr77TrpfsX3	III/2 (Fig. 1d)	family 6	fALS	Germany	ES
	c.1340+1G>A	p.Ala417X	-	family 7	fALS	Sweden	ES
	c.1340+1G>A	p.Ala417X	-	family 8	sALS	Sweden	HRMCA
	c.1340+1G>A	p.Ala417X	-	family 9	sALS	Sweden	HRMCA
	c.1340+1G>A	p.Ala417X	-	family 10	sALS	Sweden	HRMCA
	c.2138+2T>C	p.690-713del	III/2 (Fig. 1e)	family 11	fALS	Denmark	ES
	c.2138+2T>C	p.690-713del	IV/2 (Fig. 1f)	family 12	fALS	Sweden	HRMCA
in-frame deletions	c.1928_1930delAAG	p.Glu643del	-	family 13	sALS	Germany	HRMCA
	c.1928_1930delAAG	p.Glu643del	-	family 14	sALS	Germany	HRMCA
missense variants	c.140G>A	p.Arg47His	-	family 15	fALS	Germany	ES
	c.314A>G	Tyr105Ser	-	family 16	sALS	Germany	HRMCA
	c.914T>C	p.Ile305Thr		family 17	sALS	Sweden	HRMCA
	c.923G>A	p.Arg308Gln	-	family 18	sALS	Sweden	HRMCA
	c.1070G>A	p.Arg357Gln	-	family 19	fALS	Sweden	ES
	c.1676T>G	p.Met559Arg	-	family 20	fALS	Portugal	ES
	c.1712C>T	p.Ala571Val	-	family 21	sALS	Sweden	HRMCA
	c.1792A>G	p.Met598Val	-	family 22	sALS	Sweden	HRMCA
	c.2086G>A	p.Glu696Lys	-	family 23	sALS	Sweden	HRMCA

	c.2086G>A	p.Glu696Lys	-	family 24	fALS	Sweden	ES

Abbreviations: Exome sequencing (ES); High resolution melting curve analysis (HRMCA); familial ALS (fALS); sporadic ALS (sALS)

Main figure Legends

Figure 1. Pedigrees of ALS families with *TBK1* mutations for which co-segregation with disease could be assessed.

Families in (e) and (f) could be linked by a common founder 5 generations earlier. Numbering of families refers to the numbering in **Table 2**. The mutation of each family is given at top of respective pedigrees. Haplotype analysis was in agreement with a common founder of families in (e) and (f).

Figure 2. Adaptor protein binding and kinase activity of ALS-associated TBK1 mutations.

(a) Co-immunoprecipitation (Co-IP) of EGFP-OPTN and Flag-TBK1-WT or the indicated mutants from HEK293T cells using anti-Flag agarose. Precipitated proteins were analyzed by immunoblotting (IB) with the indicated antibodies.

(b) Co-IP: Flag-TBK1-WT and the indicated TBK1 mutants (as bait) were purified from HEK293T cell lysates with an anti-Flag agarose, followed by incubation with recombinant GST-OPTN.

(c) GST pull-down assay of Flag-TBK1 (as in b) from HEK293T cells using recombinant, immobilized GST-OPTN. Equal GST-OPTN protein levels were confirmed by Ponceau S staining.

(d) Flag-TBK1-WT and the indicated TBK1 mutants were co-expressed with GFP-OPTN in HEK293T cells followed by Western blot analysis. Phosphorylation of S177-OPTN was analyzed with a phospho-specific antibody (pS177).

(e) Co-IP of myc-IRF3 and Flag-TBK1-WT or the indicated mutants from HEK293T cells using anti-Flag agarose.

(f-g) Luciferase reporter assay for TBK1-induced promoter activities of IFN-inducible genes. HEK293T cells expressing Flag-TBK1-WT or the indicated mutants were harvested for Western blot analysis (f) and luciferase assay (g). The internal control was measured by β-GAL activity. Phosphorylation of IRF-3 was detected by a phospho-specific antibody (pS396).

"Δ690-713", "delA", "delAATT" and "delTG" (a-c, e-g) refer to the mutations c.2138+2T>C/p.690-713del, c.958delA/p.Thr320GlnfsX39, c.1343_1346delAATT/p.Ile450LysfsX14 and c.1434_1435delTG/p.Val479GlufsX3, respectively. Arrowheads point to Flag-TBK1-WT or truncated mutant proteins.

Figure 3. Zebrafish embryos injected with tbk1 morpholinos developed an axonopathy.

(a) Tbk1 knockdown phenotype was analysed 48 hours after fertilization in zebrafish embryos injected with translation (ATG MO) and splicing (SPL MO) blocking morpholinos compared to wild-type and control injected embryos (CTRL MO).

(b) Many Tbk1 knockdown zebrafish showed a curved tail phenotype (fixed embryos shown).

(c) Additionally, motor neuron axons were stained with SV2 and their length and branching were assessed.

(d,e) Tbk1 knockdown induced a shortening and abnormal branching of motor neuron axons. We analysed 33 embryos per group and the data represent the average ± sem.

Acknowledgements

We are indebted to the patients and their families for their participation in this project. We are grateful to our study nurse Antje Knehr and our technicians Nadine Todt, Elena Jasovskaja and Birgit Schmoll as well as the Ulm Neurology biobank team for excellent patient care and technical assistance. We also thank the many physicians who provided samples for this study, in particular Dr. L. Brättström, Karlskrona Hospital, Sweden. This work was supported in whole or in parts by grants from the German Federal Ministry of Education and Research (STRENGTH consortrium and BMBF; 01GI0704, German network for ALS research (MND-NET)), the Charcot Foundation for ALS Research (ACL, JHW), the virtual Helmholtz Institute "RNA-Dysmetabolismus in ALS and FTD" and the DFG-funded Swabian ALS Registry, the Swedish Research Council, the Swedish Brain Power Foundation, the Swedish Brain Research Foundation and the Ulla-Carin Lindquist Foundation, the Hållsten Research Foundation, the Swedish Association for the Neurologically Disabled, and the Knut and Alice Wallenberg Foundation. We would like to thank Anna-Karin Rikardsson and Ann-Charloth Nilsson for excellent technical assistance. The authors would like to thank the Exome Aggregation Consortium and the groups that provided exome variant data for comparison. A full list of contributing groups can be found athttp://exac.broadinstitute.org/about.

Material and Methods

Patients and Ethics statement. All ALS patients were diagnosed according to the EFNS Consensus criteria [17]. With informed written consent and approved by the national medical ethical review boards in accordance with the Declaration of Helsinki (WMA, 1964), EDTA blood samples were drawn from control individuals and ALS patients as well as their healthy relatives. Anonymous genotyping of healthy risk carriers (relatives of fALS patients) was performed after informed written consent and approved by the local medical ethical review boards. Patients were not informed about genetic results that were obtained for scientific purposes only, according to the written informed consent. DNA was extracted from EDTA blood samples according to standard procedures [18].

Genotyping for *SOD1* and *C9ORf72* mutations. Mutations in *SOD1* and *C9ORF72* were excluded before exome sequencing of familial ALS cases or high resolution melting curve analysis of Swedish ALS patients was performed. *SOD1* mutations were exluded by Sanger sequencing of all exons [19]. Genotyping for extended *C9ORF72* hexanucleotide repeat expansions was performed by repeat-primer PCR with Southern blot confirmation in case of PCR results suggesting a repeat expansion [20].

Whole exome sequencing and sequencing analysis

Exomes were enriched in solution and indexed with SureSelect XT Human All Exon 50Mb kits, version 3, 4 and 5 (Agilent Technologies). Sequencing was performed as 75 or 100 bp paired-end reads on HiSeq2000/2500 systems (Illumina). For exomes, we generated on average 10.1 (SD ±1.94) gigabases of sequence resulting in an average depth of coverage of 123 (SD ±24.0) with 94.4% (SD ±3.4) of the target regions covered at least 20 times. Minimal requirements for inclusion were 7 gigabases of mapped sequence and 90% of target regions covered at least 20 times. Image analysis and base calling was performed using Illumina Real Time Analysis. Reads were aligned against the human assembly hg19 (GRCh37) using Burrows-Wheeler Aligner. Multi-sample calling and filtering of all 202 cases and 2663 controls was performed with GATK (version 3.2-2) HaplotypeCaller and VariantRecalibrator as described in the GATK best practices guide (https://www.broadinstitute.org/gatk/guide/best-practices). Subsequently, variants overlapping low-complexity regions were filtered[21]. Initially, we called on average 25076 variants per exome. The VariantRecalibrator removed on average 3371 variants, the low complexity filter 215 variants leaving 21490 variants per exome.

The CMC burden test was used as implemented in the EPACTS software, version 3-2-6 (http://genome.sph.umich.edu/wiki/EPACTS). We compared 202 cases with 827 controls. Controls were comprised of healthy parents of children with various diseases, healthy control tissues of individuals with tumor diseases and 200 individuals of the KORA study. We performed principal component analysis as implemented in the PLINK software package (version 1.07)[22]. After PCA, we removed 7 outliers and subsequently used the first and second principal component as covariates for the burden tests.

Screening for TBK1 variants by high resolution melting curve analysis. We used Idaho LightScanner® high-resolution melting curve analysis (Biofire Inc.) to screen the coding regions and exon/intron boundaries of *TBK1* in 1,732 individuals. DNA was analyzed in doublets to prevent false positive signals. Samples with aberrant melting patterns were Sanger sequenced to identify the underlying variant. Oligonucleotide sequences for 20 amplicons are available on request.

Haplotype analysis. Haplotype blocks were generated using the default algorithm in the program Haploview [23]. Block definitions are based on Illumina HumanOmni2.5 array data from 500 control samples. The haplotype block spanning the *TBK1* gene comprises 36 SNP markers (from rs115725023 to rs7970355) covering a genomic region of 112.7 kb. All variant carriers were genotyped with the same Illumina HumanOmni2.5 array and the haplotypes were assigned to the specific haplotypes from the TBK1 block definition.

Zebrafish experiments. Morpholinos were purchased from Gene Tools (Philomath): standard control morpholino 5'-CCTCTTACCTCAGTTACAATTTATA-3' (CTRL MO), translation blocking morpholino (ATG MO) 5'-CCGTACTCTGCATGATGACTGTA-3' and splice blocking morpholino (SPL MO) 3'-GTAGATCCACCTGGACACACACCAC-5'. Morpholinos (4 ng) were injected in 1-2 cell stage zebrafish embryos. At 48 hours post fertilization, zebrafish were fixed with 4% PFA and motor neuron axons were stained using anti-SV2 antibody (DSHB, Iowa)[24]. The axonal length was measured in ImageJ and the average measure of the 5 last axons above the end of the yolk sac extension was calculated. We scored embryos as "embryos with abnormal branching" when two or more axons displayed abnormal branching. Protein lysates were prepared in RIPA buffer and analysed by Western blot.

Molecular modeling. The possible effects of the missense variants on TBK1 structure and function were assessed based on the TBK1 crystal structure [10]. Structural analysis was carried out using COOT [25], and figures were prepared in PyMOL (www.pymol.org). Based on the analysis, conservative amino acid replacements on the protein surface were not studied further.

Neuropathological evaluation and immunohistochemistry. Formalin fixed and paraffin embedded sections from the following areas were studied: Left frontal lobe; Right occipital lobe; Left cingulate gyrus; Right temporal lobe; Left corpus striatum; Right Thalamus; Right uncus with hippocampus; Mesencephalon; Pons; Medulla oblongata; Cervical spinal cord; and Cerebellum. All were investigated by routine staining (hematoxylin/eosin, luxol fast blue/cresyl violet, Van Gieson) and by immunohistochemistry. The immunohistochemistry were done using the Ventana® BenchMark ULTRA system. The following primary antibodies were used: anti-TBK1/NAK (1:25, CCD2 pretreatment, Cell Signaling Technology® #3013); anti-phosphoTBK1/NAK (1:25, CCD2 pretreatment, Cell Signaling Technology® #5483); anti-TDP-43 (1:100, CCD2 pretreatment, Proteintech™ 10782-2-AP); anti-phosphoTDP-43 (p409/410-1) (1:100, Citrate buffer pH 6.0 microwave pretreatment, Cosmo Bio CAC-TIP-PTD-M01); anti-p62 (1:50, CCD2 pretreatment, BD Biosciences 610832); anti-FUS (1:500, Citrate buffer pH 6.0 microwave pretreatment, Sigma HPA008784); anti-ubiquitin (1:500, CC1 pretreatment, Abcam ab7254); anti ubiquilin 2 (5F5) (1:10000, CCD2 pretreatment, Novus Biological H00029978-M03). Anti-SOD1 aa 24-39 (purified on Sulfolink coupling gel with SOD1 peptide aa 24-39 coupled, 1:500, Citrate buffer pH 6.0 microwave pretreatment, Agrisera AS09 535); Anti-SOD1 aa 131-153 (purified on Sulfolink coupling gel with SOD1 peptide aa 131-153 coupled, 1:1000, Citrate buffer pH 6.0 microwave pretreatment, Agrisera AS09 540).

Plasmids and constructs. Supplementary Table 2 summarizes all plasmids used in this study. TBK1 frameshift mutations and amino acid substitutions were introduced into pEF-BOS Flag-TBK1 wt using site directed mutagenesis (**Supplementary Table 3**). The expression vector for Flag-TBK1 Δ690-713 mutant was generated by amplifying bp 1-2066 of wt TBK1 from pEF-BOS TBK1 wt using oligonucleotides FW and RV(1) (**Supplementary Table 4**) adding a BamHI restriction site to the 5`-end. In two subsequent PCRs with oligonucleotides FW and RV(2) or RV(3), respectively, bp 2139-

2190 of wt TBK1 as well as a SalI restriction site were added to the 3`-end of the first PCR product. The resulting TBK1 fragment missing bp 2067-2138 was cloned into BamHI and SalI restriction sites of pEF-BOS Flag. The correctness of all DNA sequences was verified by sequencing.

Protein expression and purification. GST-fusion proteins were expressed in *Escherichia coli* BL21 (DE3) cells in LB medium. Expression was induced by addition of 0.2 mM IPTG and cells were incubated at 16°C overnight. Harvested cells were lysed using sonication in a lysis buffer (20 mM Tris-HCl pH 7.5, 10 mM EDTA, 5 mM EGTA, 150 mM NaCl) and the supernatant was subsequently applied to glutathione sepharose 4B beads (GE Healthcare). After several washes, fusion protein-bound beads were used directly in GST pulldown assays or GST-proteins were eluted from beads with elution buffer (10 mM glutathione, 50 mM Tris-HCl pH 8.0).

Immunoprecipitation and GST pulldown. HEK293T cells were transfected with expression constructs encoding the protein of interest using GeneJuice transfection reagent (Merck Millipore) according to the manufacturer's instructions. 36-48 h post-transfection cells were lysed in lysis buffer (50 mM HEPES pH 7.5, 150 mM NaCl, 1 mM EDTA, 1 mM EGTA, 1% Triton X-100, 25 mM NaF) supplemented with Phosphatase Inhibitor Cocktail 2 (Sigma) and protease inhibitors and supernatants (10 min, 10.000 x *g*) were incubated at 4°C for 6 h with GST-fusion protein-bound beads (GST pull down) or for 1 h with Flag- or GFP-beads (Immunoprecipitation). For immunoprecipitation GFP-Trap beads were purchased from ChromoTek and M2 anti-Flag affinity gel from Sigma. After 4 washes with lysis buffer, the beads and precipitated proteins were eluted with 2x SDS-PAGE loading buffer, boiled and loaded onto 9% SDS-PAGE gels for analysis using chemiluminescence based detection.

Luciferase reporter assay. $0{,}5 \times 10^6$ HEK293T cells were transfected with (each 0,25ug) pEF-BOS Flag-TBK1 constructs and pGL3-IFN-beta as luciferase reporter and pUT651 as β-galactosidase reporter using GeneJuice transfection reagent (Merck Millipore). At 48 h post-transfection the cells were washed with 1XPBS and lysates were subjected to luciferase assays following the manufacturer's protocol (Roche). Internal control was measured by β-galactosidase activity (Roche). Three independent experiments were performed using triplicate samples in each experiment.

Analysis of Lymphoblastoid cell lines (LCLs). Epstein-Barr virus transformed LCLs were generated from healthy controls and *TBK1* mutant ALS patients carrying the splice site mutation c.358+2C->T or the amino acid substitution R47H. Total RNA from LCLs was isolated with the RNeasy Plus Mini Kit (Qiagen, Hilden, Germany) and reverse transcription reactions were carried out using the QuantiTect Reverse Transcription Kit (Qiagen, Hilden, Germany) according to the manufacturer`s instructions. Resulting cDNA was used for subsequent PCR reactions.The region of interest of the TBK1 mRNA was amplified by PCR using oligonucleotides 5`-CCTTCGTCCAGTGGATGTTCA-3` and 5`-CACAGACTGTCC-ATCTTCCCC-3` spanning Exon 3 and 5 (322 bp fragment) and visualized on a 1% Agarose-Gel by staining with Ethidium-bromide. Quantitative real-time PCR (qRT-PCR) measurement of TBK1 mRNA was performed with a CFX96 Real-Time System (Bio-Rad) using the EXPRESS SYBR GreenER qPCR Supermix (life technologies) and oligonucleotides 5`-CGAGATGTGGTGGGTGGAATG-3` and 5`-CACA-GACTGTCCATCTTCCCC-3`. TBK1 mRNA levels were normalized relative to TBP (TATA Box Binding Protein) mRNA using oligonucleotide 5`-CCCATGACTCCCATGACC-3` and 5`-TTTACAACCA-AGATTCACTGTGG-3` for amplification and $2^{-\Delta\Delta Ct}$-method for normalization [26]. To determine the abundance of TBK1 protein, lysates of LCLs were subjected to Western blotting.

Immunocytochemistry of H4 neuronal cells. Neuroblastoma cell line H4 was cultured in DMEM (Gibco) + 10% FCS. H4 cells were transfected with pEF-BOS Flag-TBK1 plasmids using SuperFect Transfection Reagent (Qiagen, Hilden, Germany) according to the manufacturer`s instructions. 48 h post-transfection cells were washed with DPBS (Gibco), fixed for 10 min in 4% paraformaldehyde in DPBS, permeabilized for 10 min in DPBS with 100 mM Glycine and 0.1% Triton X-100 (pH 7.4) and blocked for 45 min in DBPS with 1.5% BSA and 0.1% Tween 20 (pH 7.4). Primary and secondary antibodies were diluted in DPBS and consecutively incubated for 45 min, respectively followed by extensive washing in DPBS. Cell nuclei were stained with Hoechst 33258. Pictures were acquired using a Zeiss Axio Observer A1 Microscope (HBO 100) and Axio Vision V4.8 sofware.

Antibodies used in this study. Anti-OPTN (Abcam, ab23666), anti-myc (Santa Cruz), anti-GFP (Living Colors; Clontech), anti-IRF3 (Cell signaling, #4962), anti-pIRF3 (Ser396) (Cell signaling, 4D4G), anti-FLAG M2 (Sigma), anti-Vinculin (Sigma, V9131), anti-TBK1 (Pierce, PA5-17478), anti-ß-actin (Cell signaling, #4970). The pS177 OPTN antibody was generated by immunoGlobe (as described in [15]). Secondary HRP conjugated antibodies, goat anti-mouse and goat anti-rabbit IgGs were used for immunoblotting. Secondary antibody used for ICC was goat-anti-mouse Dylight 488 (Pierce).

References

1. Kiernan, M.C. *et al.* Amyotrophic lateral sclerosis. *Lancet* **377**, 942-55 (2011).
2. Andersen, P.M. & Al-Chalabi, A. Clinical genetics of amyotrophic lateral sclerosis: what do we really know? *Nat Rev Neurol* **7**, 603-15 (2011).
3. Renton, A.E., Chio, A. & Traynor, B.J. State of play in amyotrophic lateral sclerosis genetics. *Nat Neurosci* **17**, 17-23 (2014).
4. Li, B. & Leal, S.M. Methods for detecting associations with rare variants for common diseases: application to analysis of sequence data. *Am J Hum Genet* **83**, 311-21 (2008).
5. Exome Aggregation Consortium (ExAC), C., MA (URL: http://exac.broadinstitute.org) [date (month, year) accessed]. (2014).
6. Abhinav, K. *et al.* Amyotrophic lateral sclerosis in South-East England: a population-based study. The South-East England register for amyotrophic lateral sclerosis (SEALS Registry). *Neuroepidemiology* **29**, 44-8 (2007).
7. Uenal, H. *et al.* Incidence and geographical variation of amyotrophic lateral sclerosis (ALS) in Southern Germany--completeness of the ALS registry Swabia. *PLoS One* **9**, e93932 (2014).
8. Gunnarsson, L.G., Dahlbom, K. & Strandman, E. Motor neuron disease and dementia reported among 13 members of a single family. *Acta Neurol Scand* **84**, 429-33 (1991).
9. van Blitterswijk, M. *et al.* Evidence for an oligogenic basis of amyotrophic lateral sclerosis. *Hum Mol Genet* **21**, 3776-84 (2012).
10. Larabi, A. *et al.* Crystal structure and mechanism of activation of TANK-binding kinase 1. *Cell Rep* **3**, 734-46 (2013).
11. Goncalves, A. *et al.* Functional dissection of the TBK1 molecular network. *PLoS One* **6**, e23971 (2011).
12. Ikeda, F. *et al.* Involvement of the ubiquitin-like domain of TBK1/IKK-i kinases in regulation of IFN-inducible genes. *EMBO J* **26**, 3451-62 (2007).
13. Maruyama, H. *et al.* Mutations of optineurin in amyotrophic lateral sclerosis. *Nature* **465**, 223-6 (2010).
14. Fecto, F. *et al.* SQSTM1 mutations in familial and sporadic amyotrophic lateral sclerosis. *Arch Neurol* **68**, 1440-6 (2011).
15. Wild, P. *et al.* Phosphorylation of the autophagy receptor optineurin restricts Salmonella growth. *Science* **333**, 228-33 (2011).
16. Pilli, M. *et al.* TBK-1 promotes autophagy-mediated antimicrobial defense by controlling autophagosome maturation. *Immunity* **37**, 223-34 (2012).
17. Andersen, P.M. *et al.* EFNS guidelines on the clinical management of amyotrophic lateral sclerosis (MALS)--revised report of an EFNS task force. *Eur J Neurol* **19**, 360-75 (2012).
18. Erdmann, J. *et al.* Dysfunctional nitric oxide signalling increases risk of myocardial infarction. *Nature* **504**, 432-6 (2013).
19. Andersen, P.M. *et al.* Phenotypic heterogeneity in motor neuron disease patients with CuZn-superoxide dismutase mutations in Scandinavia. *Brain* **120 (Pt 10)**, 1723-37 (1997).
20. Akimoto, C. *et al.* A blinded international study on the reliability of genetic testing for GGGGCC-repeat expansions in C9orf72 reveals marked differences in results among 14 laboratories. *J Med Genet* **51**, 419-24 (2014).
21. Li, H. Toward better understanding of artifacts in variant calling from high-coverage samples. *Bioinformatics* **30**, 2843-2851 (2014).
22. Purcell, S. *et al.* PLINK: a tool set for whole-genome association and population-based linkage analyses. *Am J Hum Genet* **81**, 559-75 (2007).
23. Barrett, J.C., Fry, B., Maller, J. & Daly, M.J. Haploview: analysis and visualization of LD and haplotype maps. *Bioinformatics* **21**, 263-5 (2005).
24. Lemmens, R. *et al.* Overexpression of mutant superoxide dismutase 1 causes a motor axonopathy in the zebrafish. *Hum Mol Genet* **16**, 2359-65 (2007).
25. Emsley, P. & Cowtan, K. Coot: model-building tools for molecular graphics. *Acta Crystallogr D Biol Crystallogr* **60**, 2126-32 (2004).

26. Livak, K.J. & Schmittgen, T.D. Analysis of relative gene expression data using real-time quantitative PCR and the 2(-Delta Delta C(T)) Method. *Methods* **25**, 402-8 (2001).

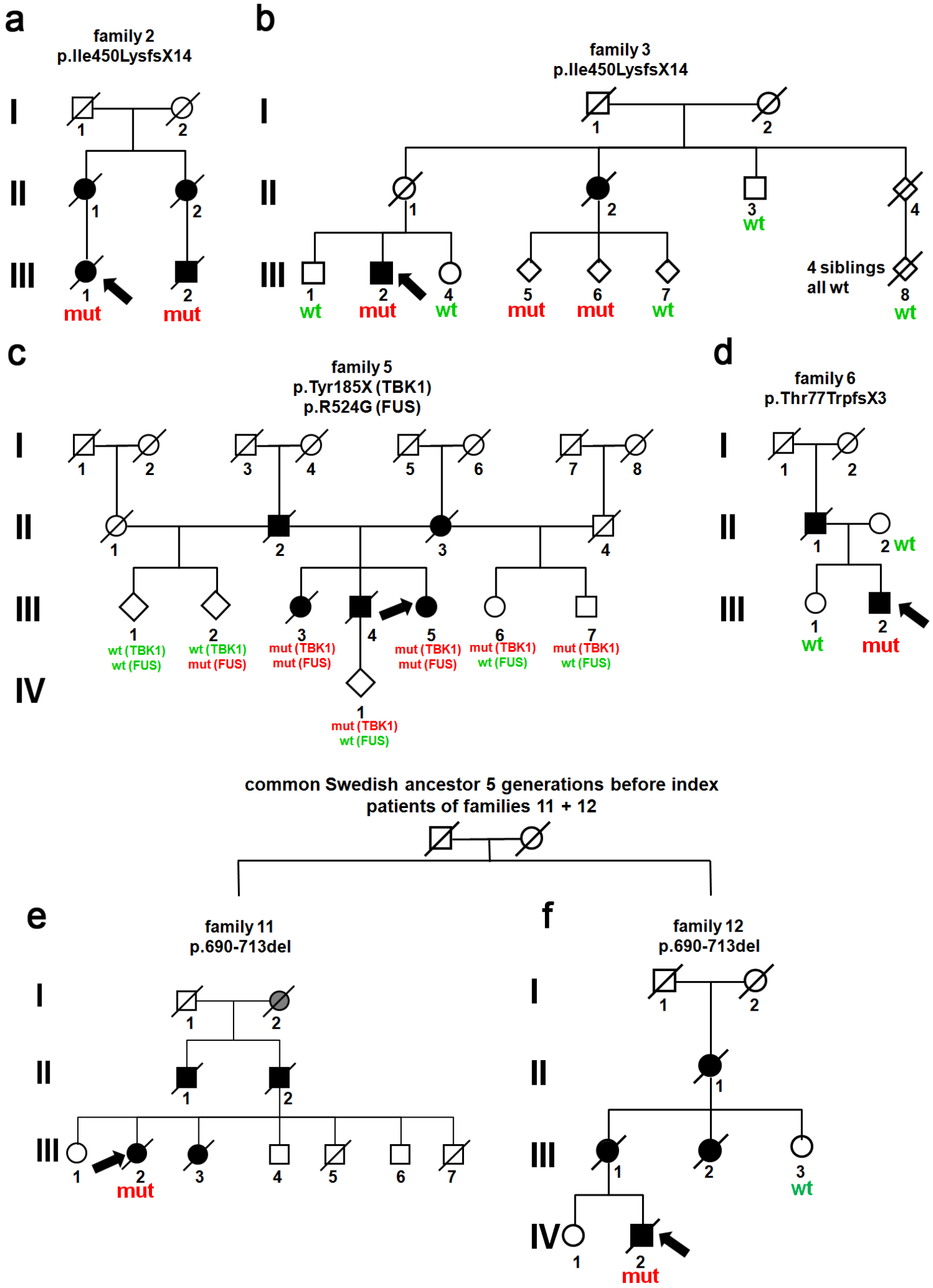
a
family 2
p.Ile450LysfsX14
I
II
III
1
2
1
2
1
2
mut
mut
b
family 3
p.Ile450LysfsX14
I
II
III
1
2
1
2
3
wt
4
1
wt
2
mut
4
wt
5
mut
6
mut
7
wt
4 siblings
all wt
8
wt
c
family 5
p.Tyr185X (TBK1)
p.R524G (FUS)
I
II
III
IV
1
2
3
4
5
6
7
8
1
2
3
4
1
wt (TBK1)
wt (FUS)
2
wt (TBK1)
mut (FUS)
3
mut (TBK1)
mut (FUS)
5
mut (TBK1)
mut (FUS)
6
mut (TBK1)
wt (FUS)
7
mut (TBK1)
wt (FUS)
1
mut (TBK1)
wt (FUS)
d
family 6
p.Thr77TrpfsX3
I
II
III
1
2
1
2 wt
1
wt
2
mut
common Swedish ancestor 5 generations before index
patients of families 11 + 12
e
family 11
p.690-713del
I
II
III
1
2
1
2
1
2
mut
3
4
5
6
7
f
family 12
p.690-713del
I
II
III
IV
1
2
1
1
2
3
wt
1
2
mut

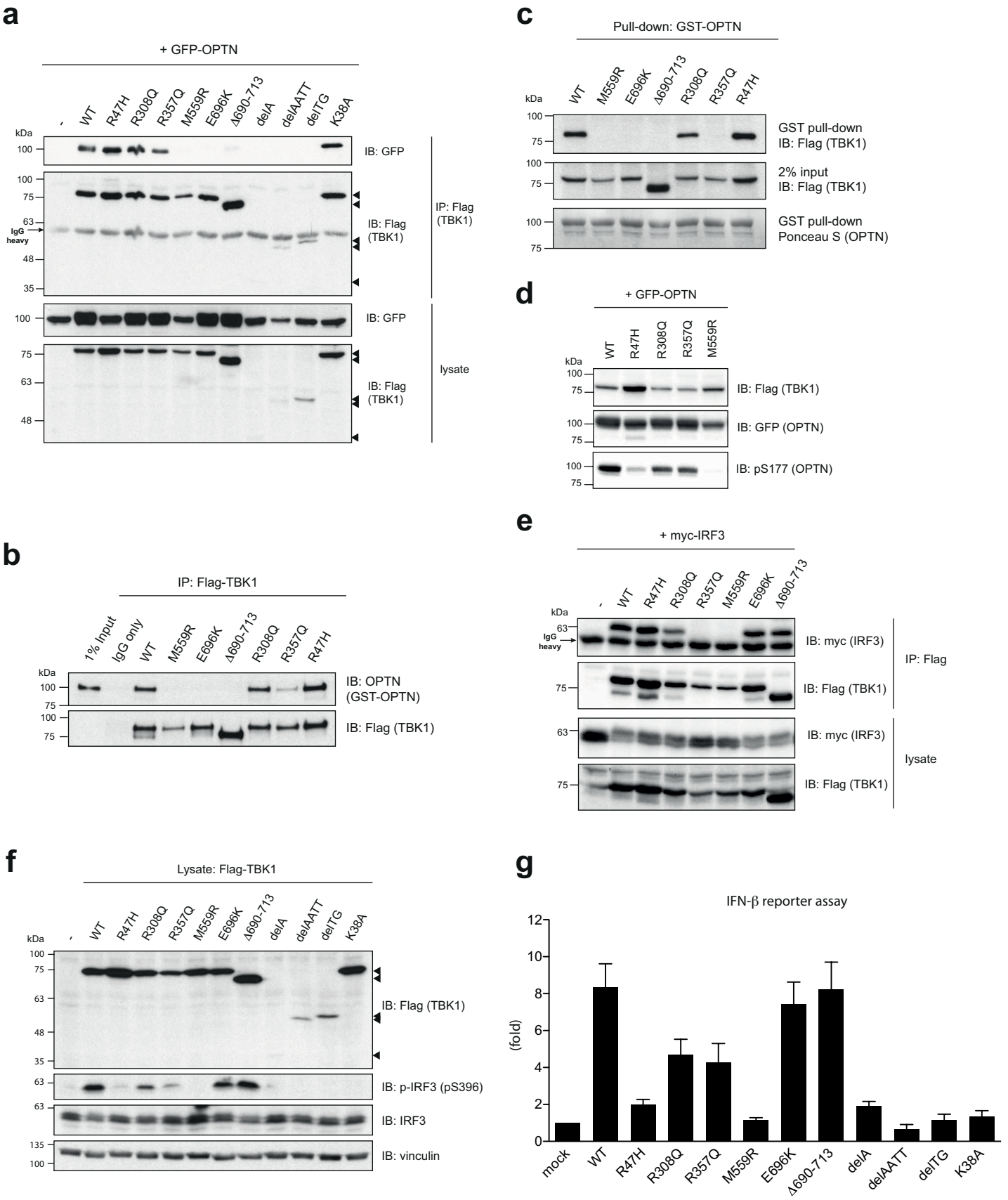
a
+ GFP-OPTN
-
WT
R47H
R308Q
R357Q
M559R
E696K
Δ690-713
delA
delAATT
delTG
K38A
kDa
IB: GFP
IB: Flag (TBK1)
IgG heavy
IP: Flag (TBK1)
lysate
b
IP: Flag-TBK1
1% Input
IgG only
IB: OPTN (GST-OPTN)
IB: Flag (TBK1)
c
Pull-down: GST-OPTN
GST pull-down IB: Flag (TBK1)
2% input IB: Flag (TBK1)
GST pull-down Ponceau S (OPTN)
d
+ GFP-OPTN
IB: Flag (TBK1)
IB: GFP (OPTN)
IB: pS177 (OPTN)
e
+ myc-IRF3
IB: myc (IRF3)
IP: Flag
lysate
f
Lysate: Flag-TBK1
IB: Flag (TBK1)
IB: p-IRF3 (pS396)
IB: IRF3
IB: vinculin
g
IFN-β reporter assay
(fold)
mock

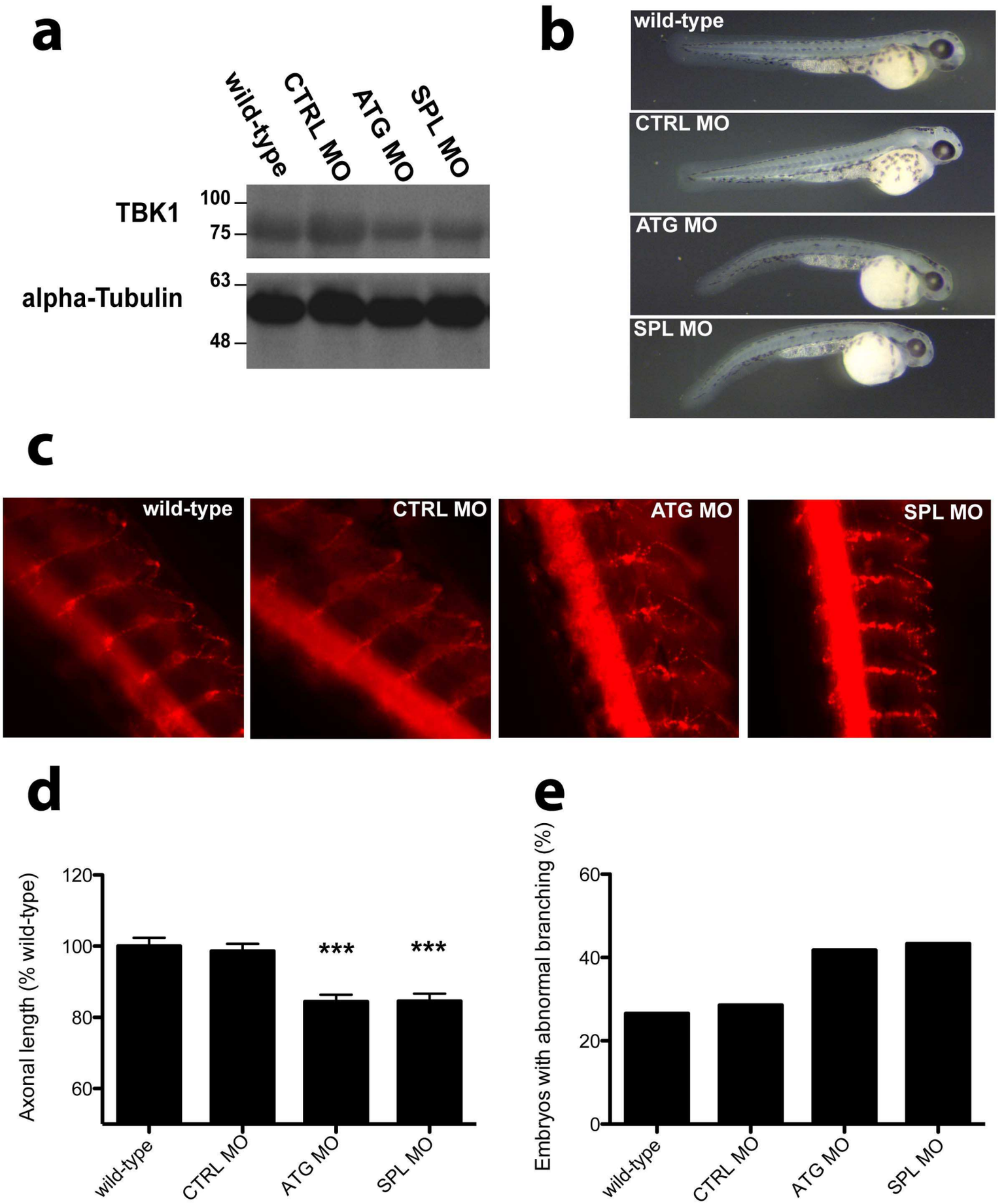
a
wild-type
CTRL MO
ATG MO
SPL MO
TBK1
100
75
alpha-Tubulin
63
48
b
wild-type
CTRL MO
ATG MO
SPL MO
c
wild-type
CTRL MO
ATG MO
SPL MO
d
Axonal length (% wild-type)
120
100
80
60
***
***
wild-type
CTRL MO
ATG MO
SPL MO
e
Embryos with abnormal branching (%)
60
40
20
0
wild-type
CTRL MO
ATG MO
SPL MO